The Gravitational Self-Force: Comparisons with Post-Newtonian Theory

Alexandre Le Tiec

University of Maryland

Methods to compute gravitational-wave templates

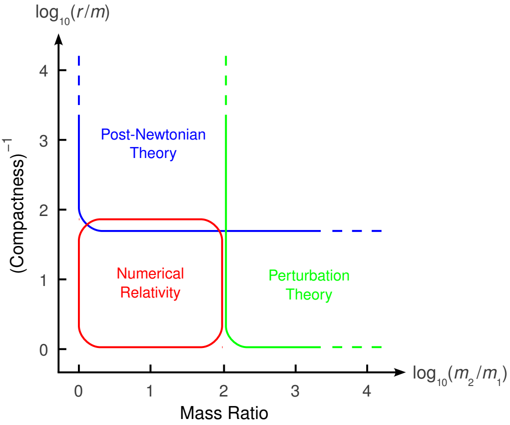

Methods to compute gravitational-wave templates

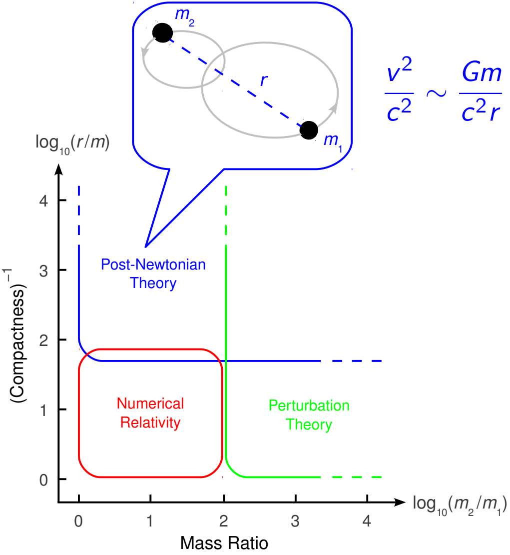

$$\frac{v^2}{c^2} \sim \frac{Gm}{c^2 r} \ll 1$$

Methods to compute gravitational-wave templates

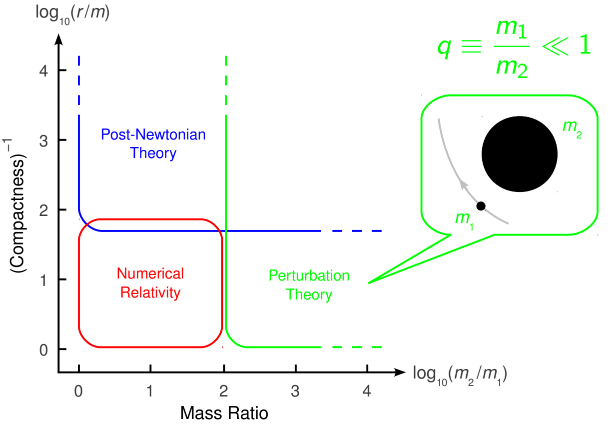

Methods to compute gravitational-wave templates

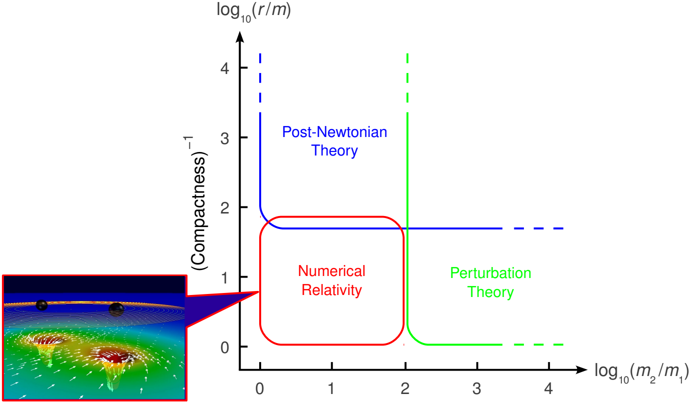

[Caltech/Cornell/CITA collaboration]

Methods to compute gravitational-wave templates

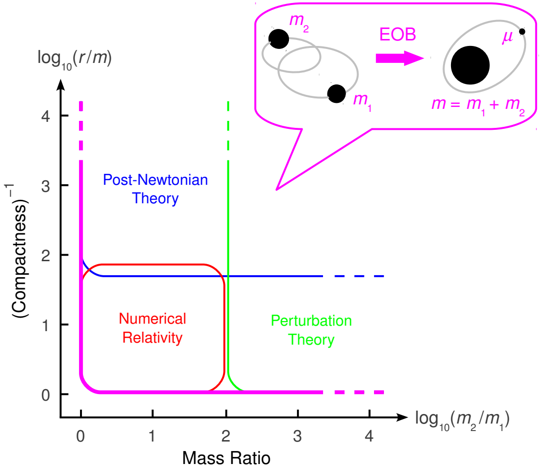

Methods to compute gravitational-wave templates

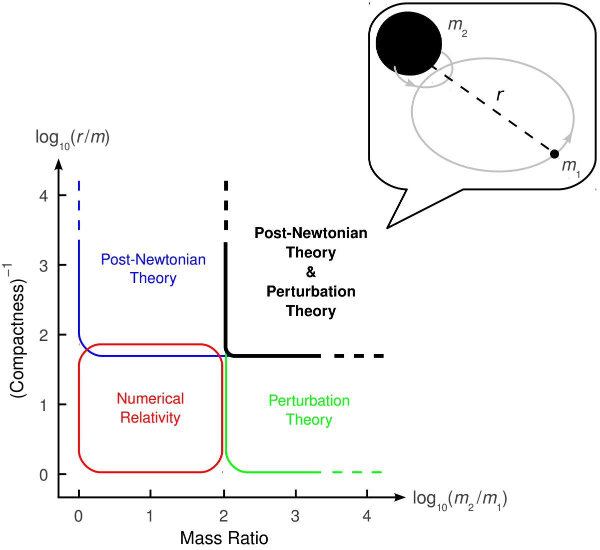

Comparing the predictions from SF analysis and PN theory

Comparing the predictions from SF analysis and PN theory

Why?

- Cross-check the validity of the various calculations
- Determine domains of validity of approximation schemes
- Test some technically simplifying assumptions
  (e.g. use of point particles + self-field regularization)
- Extract previously unknown information
  (e.g. determination of high-order PN coefficients)
- Calibration of EOB potentials

Comparing the predictions from SF analysis and PN theory

Why?

- Cross-check the validity of the various calculations
- Determine domains of validity of approximation schemes
- Test some technically simplifying assumptions
  (e.g. use of point particles + self-field regularization)
- Extract previously unknown information
  (e.g. determination of high-order PN coefficients)
- Calibration of EOB potentials

How?

✘ Use the same coordinate system in all calculations

✔ Use coordinate invariant relations to avoid gauge ambiguities

Outline

1. Dissipative SF and comparison with PN theory
2. Innermost stable circular orbit
3. Periastron advance for circular orbits
4. Redshift observable for circular orbits
5. Redshift observable for eccentric orbits

Self-force vs post-Newtonian mass conventions

	SF	PN
mass of the “particle”	μ	m_1
mass of the “black hole”	M	m_2
total mass	$\mu + M \simeq M$	$m = m_1 + m_2$
reduced mass	$\frac{\mu M}{\mu + M} \simeq \mu$	$\mu = \frac{m_1 m_2}{m}$
symmetric mass ratio	$\frac{\mu M}{(\mu + M)^2} \simeq \frac{\mu}{M}$	$\nu = \frac{m_1 m_2}{m^2}$
(asymmetric) mass ratio	$\frac{\mu}{M} \ll 1$	$q = \frac{m_1}{m_2}$

We shall use the PN mass conventions

Outline

1. Dissipative SF and comparison with PN theory
2. Innermost stable circular orbit
3. Periastron advance for circular orbits
4. Redshift observable for circular orbits
5. Redshift observable for eccentric orbits

PN equations of motion for compact binaries

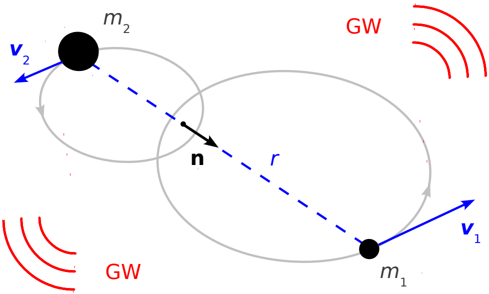

$$\frac{\mathrm{d}\mathbf{v}_1}{\mathrm{d}t} = \underbrace{-\frac{Gm_2}{r^2}\mathbf{n} + \frac{\mathbf{A}_{1\mathrm{PN}}}{c^2} + \frac{\mathbf{A}_{2\mathrm{PN}}}{c^4}}_{\text{conservative terms}} + \underbrace{\frac{\mathbf{A}_{2.5\mathrm{PN}}}{c^5}}_{\text{rad. reac.}} + \underbrace{\frac{\mathbf{A}_{3\mathrm{PN}}}{c^6}}_{\text{cons. term}} + \underbrace{\frac{\mathbf{A}_{3.5\mathrm{PN}}}{c^7}}_{\text{rad. reac.}} + \cdots$$

Templates for circularized inspiralling compact binaries

- Conservative part of the orbital dynamics yields center of mass binding energy

$$E = \underbrace{-\frac{1}{2}\mu\left(m\Omega_\varphi\right)^{2/3}}_{\substack{\text{Newtonian}\\ \text{binding energy}}}\left\{1 + (\text{PN corrections})\right\}$$

- Wave generation formalism yields binary's GW energy flux

$$\mathcal{F} = \underbrace{\frac{32}{5}\nu^2\left(m\Omega_\varphi\right)^5}_{\substack{\text{Einstein's}\\ \text{quadrupole formula}}}\left\{1 + (\text{PN corrections})\right\}$$

- Orbital phase $\varphi(t)$ then GW phase follow from energy balance

$$\frac{\mathrm{d}E}{\mathrm{d}t} = -\mathcal{F}$$

Energy loss caused by the dissipative SF

- Energy balance for a point particle orbiting a Schwarzschild black hole (BH) on quasi-circular orbits

$$\underbrace{\mathcal{F}_\infty}_{\substack{\text{GW flux}\\ \text{at infinity}}} + \underbrace{\mathcal{F}_\bullet}_{\substack{\text{GW flux}\\ \text{through BH}}} = \underbrace{-\frac{m_1}{2u^t} u^\alpha u^\beta \partial_t h_{\alpha\beta}}_{\substack{\text{work done by the}\\ \text{gravitational SF}}}$$

- $\mathcal{F}_\bullet$ is a 4PN effect relative to $\mathcal{F}_\infty$ [Poisson & Sasaki 1995]

$$\frac{\mathcal{F}_\bullet}{\mathcal{F}_\infty} = \underbrace{(m_2\Omega_\varphi)^{8/3}}_{\sim v^8} \left\{ 1 + (\text{PN corrections}) \right\}$$

- Beyond the ISCO, it is numerically small [Martel 2004]

$$\mathcal{F}_\bullet \lesssim 10^{-3}\, \mathcal{F}_\infty$$

$\mathcal{F}_\infty$ effectively measures the dissipative component of the SF

Perturbative GW energy flux calculations

- For a test particle (geodesic motion) in circular orbit around a Schwarzschild BH, $\mathcal{F}_\infty$ has been computed analytically to:
  - 1.5PN order beyond $\mathcal{F}_\text{N}$ [Poisson 1993]
  - 4PN [Tagoshi & Sasaki 1994]
  - 5.5PN [Tanaka, Tagoshi & Sasaki 1996]
  - 14PN [Fujita 2011]

$$\mathcal{F}_\infty = \underbrace{\frac{32}{5} q^2 \left(m_2 \Omega_\varphi\right)^5}_{\text{Newtonian flux } \mathcal{F}_\text{N}} \left\{ 1 + (\text{PN corrections}) \right\}$$

- 3.5PN restriction agrees with limit $q \to 0$ of PN result $\mathcal{F}$
- Similar results for eccentric orbits and/or Kerr black holes

Dissipative part of the SF successfully tested against PN theory

More recently, comparisons between PN and the **conservative** SF

Outline

1. Dissipative SF and comparison with PN theory
2. Innermost stable circular orbit
3. Periastron advance for circular orbits
4. Redshift observable for circular orbits
5. Redshift observable for eccentric orbits

SF correction to the location of the Schwarzschild ISCO

$$m\Omega_{\text{ISCO}} = \underbrace{6^{-3/2}}_{\substack{\text{Schwarz.}\\ \text{result}}} \left\{ 1 + \underbrace{q\, c_\Omega}_{\substack{\text{conservative}\\ \text{SF correction}}} + \mathcal{O}(q^2) \right\}$$

- In the Lorenz gauge, the self-force analysis yields [Barack & Sago 2009]

$$c_\Omega^{\text{BS}} = 1.4870(6)$$

- In a gauge such that $g_{\alpha\beta} \to \eta_{\alpha\beta}$ at spatial infinity [Damour 2010]

$$c_\Omega = c_\Omega^{\text{BS}} - \frac{1}{\sqrt{18}} = 1.2513(6)$$

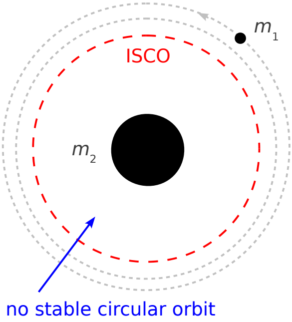

Comparison with multiple PN/EOB approximants

[Favata 2010]

Method	$c_\Omega^{\rm PN}$
A4PN-P$_A$	1.132
A4PN-T$_A$	1.132
$C_0$3PN	1.435
e2PN-P	1.036
KWW-1PN	1.592
A3PN-P	0.9067
A3PN-T	0.9067
A4PN-P$_B$	0.8419
A4PN-T$_B$	0.8419
j3PN-P	1.711
j2PN-P	0.6146
KWW-S	0.5610
$C_0$2PN	0.5833
E_h3PN	0.4705
e3PN-P	2.178
A2PN-P	0.2794
A2PN-T	0.2794
E_h2PN	0.0902
E_h1PN	−0.014 73
E_h-S	−0.054 71
HH-S	−0.1486
j1PN-P	−0.1667
KWW-2PN	−1.542
j-P-S	−2.104
KWW-3PN	4.851
HH-1PN	6.062
HH-2PN	−12.75
HH-3PN	25.42

$$c_\Omega = 1.2513(6)$$

Comparison with multiple PN/EOB approximants

[Favata 2010]

Method	$c_\Omega^{\rm PN}$
A4PN-P$_A$	1.132
A4PN-T$_A$	1.132
$C_0$3PN	1.435
e2PN-P	1.036
KWW-1PN	1.592
A3PN-P	0.9067
A3PN-T	0.9067
A4PN-P$_B$	0.8419
A4PN-T$_B$	0.8419
j3PN-P	1.711
j2PN-P	0.6146
KWW-S	0.5610
$C_0$2PN	0.5833
E_h3PN	0.4705
e3PN-P	2.178
A2PN-P	0.2794
A2PN-T	0.2794
E_h2PN	0.0902
E_h1PN	−0.014 73
E_h-S	−0.054 71
HH-S	−0.1486
j1PN-P	−0.1667
KWW-2PN	−1.542
j-P-S	−2.104
KWW-3PN	4.851
HH-1PN	6.062
HH-2PN	−12.75
HH-3PN	25.42

$$c_\Omega = 1.2513(6)$$

- EOB with NR calibration of the 4PN coefficient a_5 agrees best (10% error)

Comparison with multiple PN/EOB approximants

[Favata 2010]

Method	c_Ω^{PN}
A4PN-P$_A$	1.132
A4PN-T$_A$	1.132
$C_0$3PN	1.435
e2PN-P	1.036
KWW-1PN	1.592
A3PN-P	0.9067
A3PN-T	0.9067
A4PN-P$_B$	0.8419
A4PN-T$_B$	0.8419
j3PN-P	1.711
j2PN-P	0.6146
KWW-S	0.5610
$C_0$2PN	0.5833
E_h3PN	0.4705
e3PN-P	2.178
A2PN-P	0.2794
A2PN-T	0.2794
E_h2PN	0.0902
E_h1PN	−0.014 73
E_h-S	−0.054 71
HH-S	−0.1486
j1PN-P	−0.1667
KWW-2PN	−1.542
j-P-S	−2.104
KWW-3PN	4.851
HH-1PN	6.062
HH-2PN	−12.75
HH-3PN	25.42

$$c_\Omega = 1.2513(6)$$

- EOB with NR calibration of the 4PN coefficient a_5 agrees best (10% error)
- However uncalibrated EOB 3PN performs three times worse (28% error)

Comparison with multiple PN/EOB approximants

[Favata 2010]

Method	$c_{\Omega}^{\rm PN}$
A4PN-P$_A$	1.132
A4PN-T$_A$	1.132
$\boxed{C_0\text{3PN}}$	$\boxed{1.435}$
e2PN-P	1.036
KWW-1PN	1.592
A3PN-P	0.9067
A3PN-T	0.9067
A4PN-P$_B$	0.8419
A4PN-T$_B$	0.8419
j3PN-P	1.711
j2PN-P	0.6146
KWW-S	0.5610
$C_0$2PN	0.5833
E_h3PN	0.4705
e3PN-P	2.178
A2PN-P	0.2794
A2PN-T	0.2794
E_h2PN	0.0902
E_h1PN	−0.014 73
E_h-S	−0.054 71
HH-S	−0.1486
j1PN-P	−0.1667
KWW-2PN	−1.542
j-P-S	−2.104
KWW-3PN	4.851
HH-1PN	6.062
HH-2PN	−12.75
HH-3PN	25.42

$$c_{\Omega} = 1.2513(6)$$

- EOB with NR calibration of the 4PN coefficient a_5 agrees best (10% error)
- However uncalibrated EOB 3PN performs three times worse (28% error)
- The only non-resummed method, based on a stability analysis of the 3PN EOM, is in good agreement (15% error)

Comparison with multiple PN/EOB approximants

[Favata 2010]

Method	$c_\Omega^{\rm PN}$
A4PN-P$_A$	1.132
A4PN-T$_A$	1.132
$\boxed{C_0\text{3PN}}$	$\boxed{1.435}$
e2PN-P	1.036
KWW-1PN	1.592
A3PN-P	0.9067
A3PN-T	0.9067
A4PN-P$_B$	0.8419
A4PN-T$_B$	0.8419
j3PN-P	1.711
j2PN-P	0.6146
KWW-S	0.5610
$C_0$2PN	0.5833
E_h3PN	0.4705
e3PN-P	2.178
A2PN-P	0.2794
A2PN-T	0.2794
E_h2PN	0.0902
E_h1PN	−0.014 73
E_h-S	−0.054 71
HH-S	−0.1486
j1PN-P	−0.1667
KWW-2PN	−1.542
j-P-S	−2.104
KWW-3PN	4.851
HH-1PN	6.062
HH-2PN	−12.75
HH-3PN	25.42

$$c_\Omega = 1.2513(6)$$

- EOB with NR calibration of the 4PN coefficient a_5 agrees best (10% error)
- However uncalibrated EOB 3PN performs three times worse (28% error)
- The only non-resummed method, based on a stability analysis of the 3PN EOM, is in good agreement (15% error)
- It also reproduces the exact result in the test-particle limit: $m\Omega_{\rm ISCO} = 6^{-3/2}$

Outline

1. Dissipative SF and comparison with PN theory
2. Innermost stable circular orbit
3. Periastron advance for circular orbits
4. Redshift observable for circular orbits
5. Redshift observable for eccentric orbits

Periastron advance in black hole binaries

- Conservative part of the dynamics only
- Generic non-circular orbit parametrized by the two invariant frequencies

$$\Omega_r = \frac{2\pi}{P}\,, \quad \Omega_\varphi = \frac{1}{P}\int_0^P \dot{\varphi}(t)\,\mathrm{d}t$$

- Periastron advance per radial period

$$K \equiv \frac{\Omega_\varphi}{\Omega_r} = 1 + \frac{\Delta\Phi}{2\pi}$$

- In the circular orbit limit $e \to 0$, the relation $K(\Omega_\varphi)$ is coordinate invariant

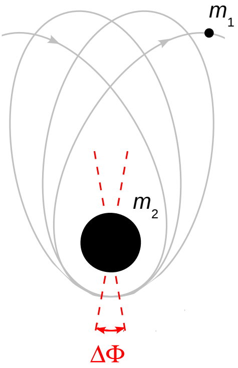

SF correction to the Schwarzschild periastron advance

- In the extreme mass ratio limit $q \ll 1$:

$$W \equiv \frac{1}{K^2} = \underbrace{1 - 6x}_{\text{Schw.}} + \underbrace{q\,\rho(x)}_{\text{SF effect}} + \mathcal{O}(q^2)\,,$$

  where $x \equiv (m\Omega_\varphi)^{2/3}$

- The gravitational SF correction $\rho(x)$ has recently been computed numerically [Barack & Sago 2010]
- The PN expansion of $\rho(x)$ is known up to 3PN order, as well as the leading order 4PN and next-to-leading order 5PN logarithmic contributions [Damour 2010]

Comparison of the PN and SF results

[Barack, Damour & Sago 2010]

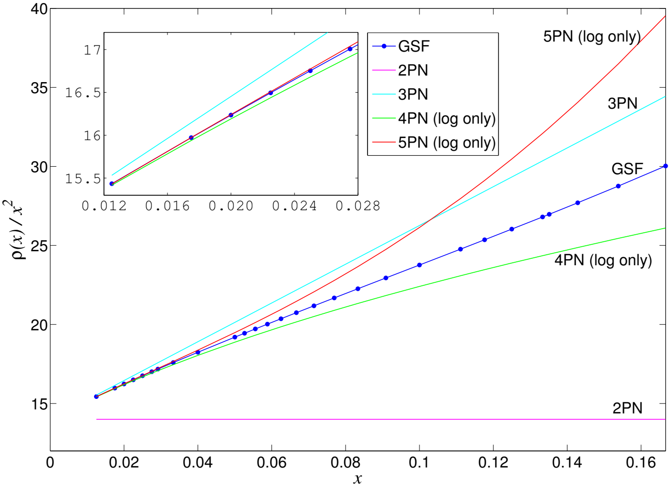

Comparison with numerical relativity

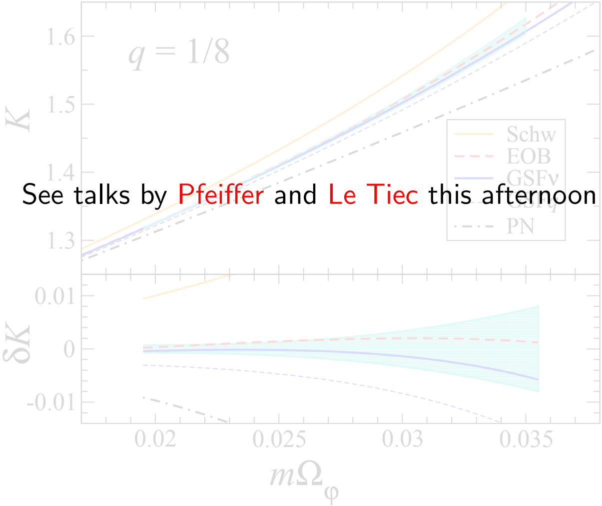

See talks by Pfeiffer and Le Tiec this afternoon

Outline

The "redshift observable" for circular orbits

- Conservative part of the dynamics only
- For circular orbits, the geometry admits an helical Killing vector k^α such that

$$k^\alpha = (\partial_t)^\alpha + \Omega_\varphi \, (\partial_\varphi)^\alpha \quad \text{(asymptotically)}$$

- Four-velocity u_1^α of the particle necessarily tangent to the helical Killing vector:

$$u_1^\alpha = U \, k_1^\alpha$$

- Relation $U(\Omega_\varphi)$ well defined in PN and SF frameworks, and coordinate invariant

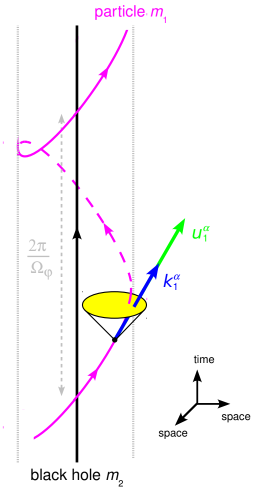

Physical interpretations of the quantity U

- It measures the redshift of light rays emitted from the particle [Detweiler 2008]

$$\frac{\mathcal{E}_{\text{obs}}}{\mathcal{E}_{\text{em}}} \equiv \frac{(p_\alpha u^\alpha_{\text{obs}})_B}{(p_\alpha u^\alpha_{\text{em}})_A} = \frac{1}{U}$$

- It is a constant of the motion associated with the helical symmetry

$$u_{1\alpha} k^\alpha_1 = -\frac{1}{U}$$

- In a gauge such that $k^\alpha \partial_\alpha = \partial_t + \Omega_\varphi \, \partial_\varphi$ everywhere, we simply have

$$U = u^t_1$$

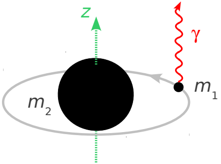

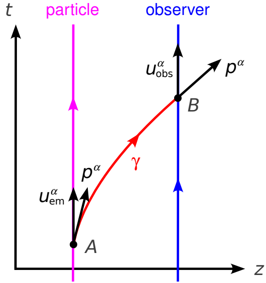

Post-Newtonian result for the SF effect on $U(\Omega_\varphi)$

[Detweiler 2008; Blanchet, Detweiler, Le Tiec & Whiting 2010 (a,b)]

- In the extreme mass ratio limit $q \ll 1$:

$$U = U_{\text{Schw}} \underbrace{- q\, U_{\text{SF}}}_{\text{SF effect}} + \mathcal{O}(q^2)$$

- PN result expressed as a power series in $y \equiv (m_2 \Omega_\varphi)^{2/3} \sim v^2$:

$$U_{\text{SF}} = y + 2y^2 + 5y^3 + \overbrace{\left(\frac{121}{3} - \frac{41}{32}\pi^2\right) y^4}^{\text{3PN contribution}}$$
$$+ \left(\alpha_4 + \underbrace{\frac{64}{5} \ln y}_{\text{4PN log}}\right) y^5 + \left(\alpha_5 \underbrace{- \frac{956}{105} \ln y}_{\text{5PN log}}\right) y^6 + o(y^6)$$

- The 4PN and 5PN polynomial coefficients $\{\alpha_4, \alpha_5\}$ are unknown, but can be extracted from the SF calculation

High-precision comparison of the 3PN coefficient

- The result of the SF calculation is fitted by a PN series

$$U_{\mathrm{SF}} = \sum_{n\geqslant 0} \alpha_n \, y^{n+1} + \ln y \sum_{n\geqslant 4} \beta_n \, y^{n+1}$$

High-precision comparison of the 3PN coefficient

- The result of the SF calculation is fitted by a PN series

$$U_{\mathrm{SF}} = \sum_{n\geqslant 0} \alpha_n\, y^{n+1} + \ln y \sum_{n\geqslant 4} \beta_n\, y^{n+1}$$

- The known values of the coeffs. $\{\alpha_0, \alpha_1, \alpha_2\}$ up to 2PN are used, as well as the 4PN and 5PN logarithmic coeffs. $\{\beta_4, \beta_5\}$

High-precision comparison of the 3PN coefficient

- The result of the SF calculation is fitted by a PN series

$$U_{\mathrm{SF}} = \sum_{n\geqslant 0} \alpha_n \, y^{n+1} + \ln y \sum_{n\geqslant 4} \beta_n \, y^{n+1}$$

- The known values of the coeffs. $\{\alpha_0, \alpha_1, \alpha_2\}$ up to 2PN are used, as well as the 4PN and 5PN logarithmic coeffs. $\{\beta_4, \beta_5\}$
- The fit of the numerical SF data yields for the 3PN coefficient

$$\alpha_3^{\mathrm{fit}} = 27.6879035 \pm 0.0000004$$

High-precision comparison of the 3PN coefficient

- The result of the SF calculation is fitted by a PN series

$$U_{\mathrm{SF}} = \sum_{n\geqslant 0} \alpha_n \, y^{n+1} + \ln y \sum_{n\geqslant 4} \beta_n \, y^{n+1}$$

- The known values of the coeffs. $\{\alpha_0, \alpha_1, \alpha_2\}$ up to 2PN are used, as well as the 4PN and 5PN logarithmic coeffs. $\{\beta_4, \beta_5\}$
- The fit of the numerical SF data yields for the 3PN coefficient

$$\alpha_3^{\mathrm{fit}} = 27.6879035 \pm 0.0000004$$

- To be compared with the exact analytical result

$$\alpha_3 = \frac{121}{3} - \frac{41}{32}\pi^2 = 27.6879026\cdots$$

High-precision comparison of the 3PN coefficient

- The result of the SF calculation is fitted by a PN series

$$U_{\mathrm{SF}} = \sum_{n\geqslant 0} \alpha_n\, y^{n+1} + \ln y \sum_{n\geqslant 4} \beta_n\, y^{n+1}$$

- The known values of the coeffs. $\{\alpha_0, \alpha_1, \alpha_2\}$ up to 2PN are used, as well as the 4PN and 5PN logarithmic coeffs. $\{\beta_4, \beta_5\}$
- The fit of the numerical SF data yields for the 3PN coefficient

$$\alpha_3^{\mathrm{fit}} = 27.6879035 \pm 0.0000004$$

- To be compared with the exact analytical result

$$\alpha_3 = \frac{121}{3} - \frac{41}{32}\pi^2 = 27.6879026\cdots$$

- The two calculations are therefore in agreement at the 2σ level with 9 significant digits

High-order PN fit of the gravitational SF calculation

- The result of the SF calculation is fitted by a PN series

$$U_{\mathrm{SF}} = \sum_{n\geqslant 0} \alpha_n \, y^{n+1} + \ln y \sum_{n\geqslant 4} \beta_n \, y^{n+1}$$

- The know value of the 3PN coefficient α_3 is also included
- The best fit yields:

PN order	Coeff.	Value
4	α_4	$+114.34747(5)$
5	α_5	$+245.53(1)$
6	α_6	$+695(2)$
6	β_6	$-339.3(5)$
7	α_7	$+5837(16)$

Comparison of the PN and SF results

[Blanchet, Detweiler, Le Tiec & Whiting 2010 (a,b)]

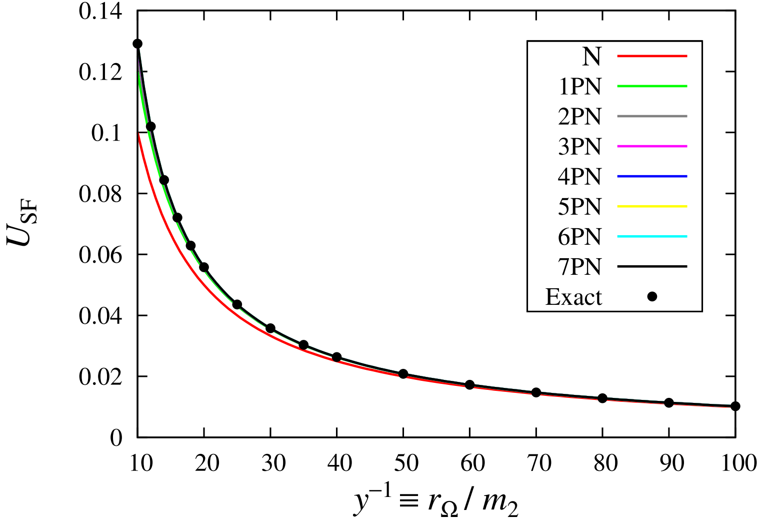

Comparison of the PN and SF results

[Blanchet, Detweiler, Le Tiec & Whiting 2010 (a,b)]

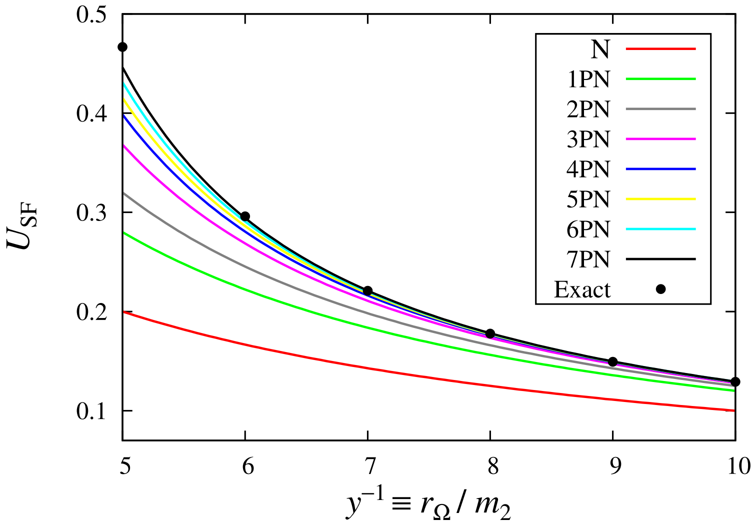

Comparison of the PN and SF results

[Blanchet, Detweiler, Le Tiec & Whiting 2010 (a,b)]

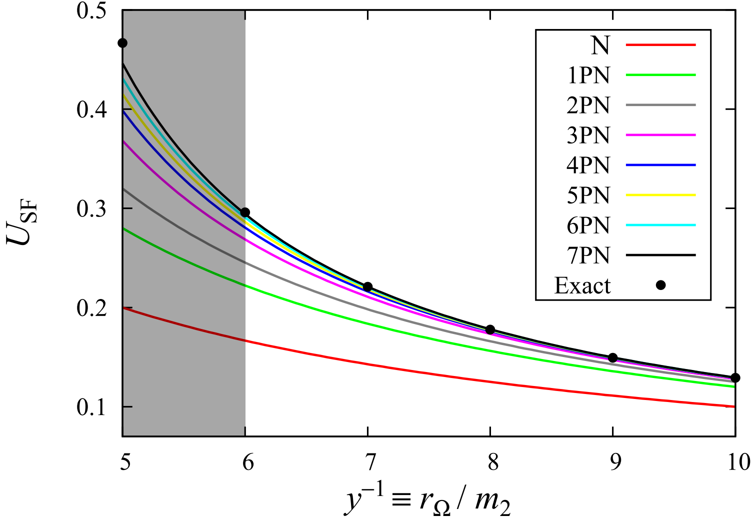

Outline

Averaged "redshift observable" for eccentric orbits

- Conservative part of the dynamics only
- Generic eccentric orbit parametrized by the two invariant frequencies

$$\Omega_r = \frac{2\pi}{P}\,, \quad \Omega_\varphi = K\,\Omega_r$$

- Averaging of U with respect to proper time τ over one radial period:

$$\langle U \rangle \equiv \frac{1}{T}\int_0^T U(\tau)\,\mathrm{d}\tau = \frac{P}{T}$$

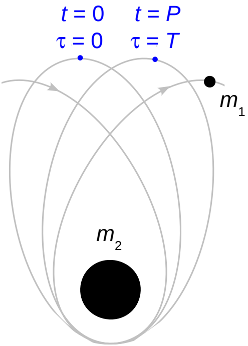

- Relation $\langle U \rangle(\Omega_r, \Omega_\varphi)$ well defined in both PN and SF frameworks, and coordinate invariant

PN calculation of the invariant relation $\langle U\rangle(\Omega_r, \Omega_\varphi)$

- Compute the PN expansion of the combination

$$U = \left[g_{\alpha\beta}(y_1)\, v_1^\alpha v_1^\beta\right]^{-1/2} ,$$

  where $g_{\alpha\beta}(y_1)$ is the regularized metric at the location y_1 of the particle m_1
- Express the result in the center-of-mass frame
- Use the generalized quasi-Keplerian representation of the motion [Memmesheimer, Gopakumar & Schäfer (2004)]
- Compute the orbital average $\langle U\rangle$ over one radial period
- Express the result in terms of the frequencies Ω_r and Ω_φ

2PN result for the invariant relation $\langle U\rangle(\Omega_r, \Omega_\varphi)$

[Barack, Le Tiec & Sago (work in progress)]

- Result expressed as a power series in $x \equiv (m\Omega_\varphi)^{2/3} \sim v^2$:

$$\langle U\rangle = 1 + A_0\, x + A_1\, x^2 + A_2\, x^3 + \mathcal{O}(x^4)$$

- Coefficients $A_k(\iota;\nu)$ depend on $\iota \equiv 3x/(K-1) \sim 1 - e^2$:

$$A_0 = \frac{3}{4} + \frac{3}{4}\Delta - \frac{\nu}{2}$$

$$A_1 = \frac{3}{16} + \frac{3}{16}\Delta - \frac{7}{2}\nu - \frac{5}{8}\Delta\,\nu + \frac{\nu^2}{24} + \frac{3+3\Delta}{\sqrt{\iota}} - \frac{3+3\Delta-2\nu}{2\iota}$$

$$A_2 = -\frac{41}{32} + \frac{41}{32}\Delta + \frac{3}{4}\nu + \frac{43}{16}\Delta\,\nu - \frac{99}{32}\nu^2 - \frac{5}{32}\Delta\,\nu^2 - \frac{\nu^3}{48} + \left(\frac{57}{8} + \frac{57}{8}\Delta - 22\nu - \frac{3}{2}\Delta\,\nu - 2\nu^2\right)\frac{1}{\sqrt{\iota}} + \cdots$$

2PN result for the SF effect on $\langle U \rangle(\Omega_r, \Omega_\varphi)$

- In the extreme mass ratio limit $q \ll 1$:

$$\langle U \rangle = \langle U \rangle_{\text{Schw}} \underbrace{- q \, \langle U \rangle_{\text{SF}}}_{\text{SF effect}} + \mathcal{O}(q^2)$$

- The first order correction $\langle U \rangle_{\text{SF}}(\Omega_r, \Omega_\varphi)$ is computed numerically within the SF analysis [Barack & Sago 2011]
- The 2PN approximation to this exact result reads

$$\langle U \rangle_{\text{SF}} = y + \left(4 - \frac{2}{\sqrt{\lambda}}\right) y^2 + \left(6 + \frac{14}{\sqrt{\lambda}} - \frac{16}{\lambda} + \frac{5}{\lambda^{3/2}} + \frac{5}{\lambda^2}\right) y^3 + \mathcal{O}(y^4) \, ,$$

where $y \equiv (m_2 \Omega_\varphi)^{2/3} \sim v^2$ and $\lambda \equiv 3y/(K-1) \sim 1 - e^2$

Usual parametrization of BH perturbation theory

- Parametrization in terms of coordinate dependant semi-latus rectum p and eccentricity e, defined such that

$$r(\chi) = \frac{p\, m_2}{1 + e \cos \chi}\,, \quad \chi \in [0, 2\pi]$$

- Stable bound geodesic orbits for $0 \leqslant e < 1$ and $p > 6 + 2e$ [Cutler, Kennefick & Poisson 1994]

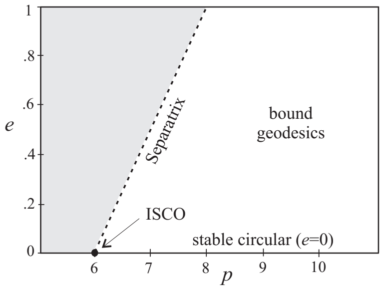

Comparison of the PN and SF results

[Barack, Le Tiec & Sago (work in progress)]

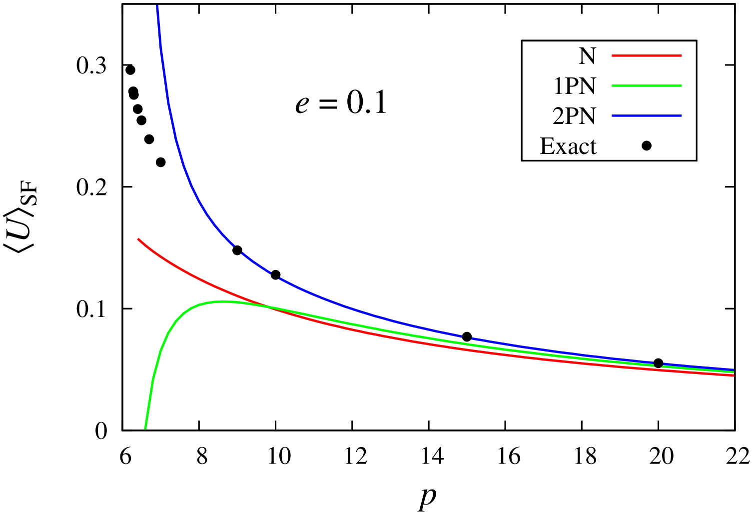

Comparison of the PN and SF results

[Barack, Le Tiec & Sago (work in progress)]

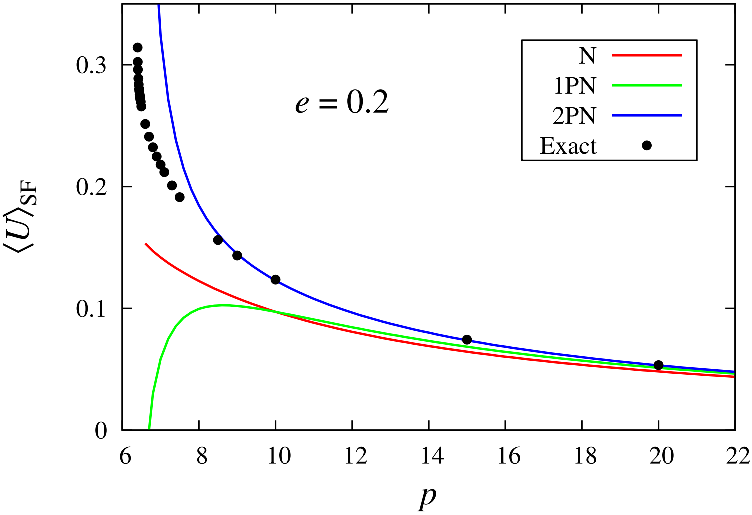

Comparison of the PN and SF results

[Barack, Le Tiec & Sago (work in progress)]

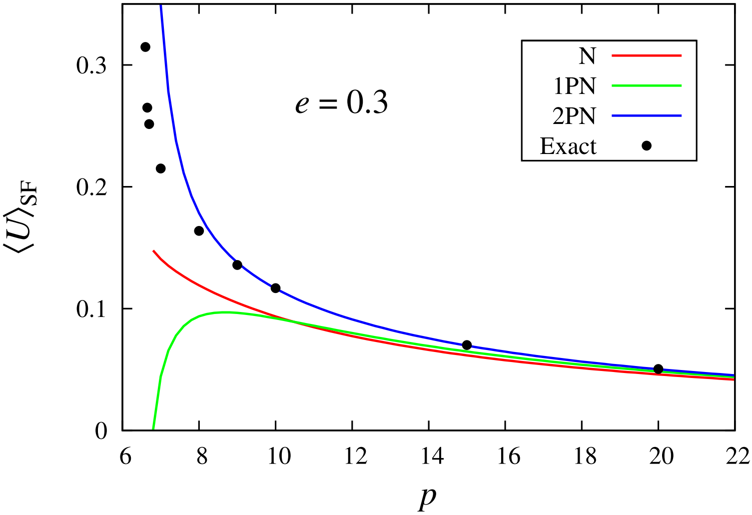

Comparison of the PN and SF results

[Barack, Le Tiec & Sago (work in progress)]

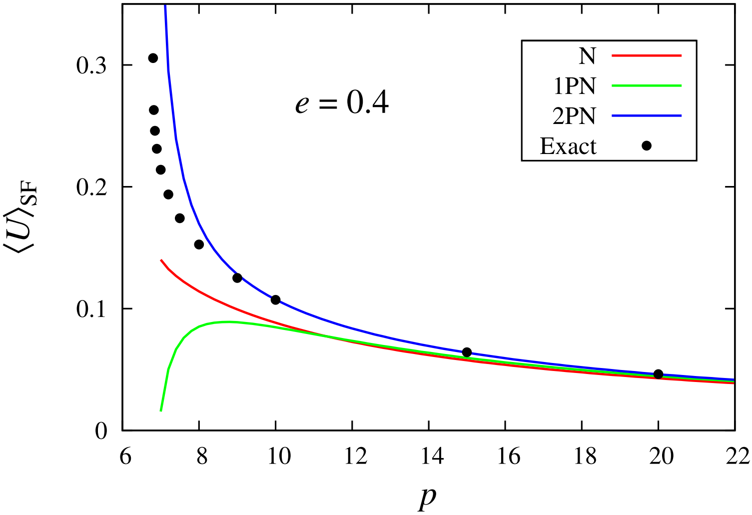

Comparison of the PN and SF results

[Barack, Le Tiec & Sago (work in progress)]

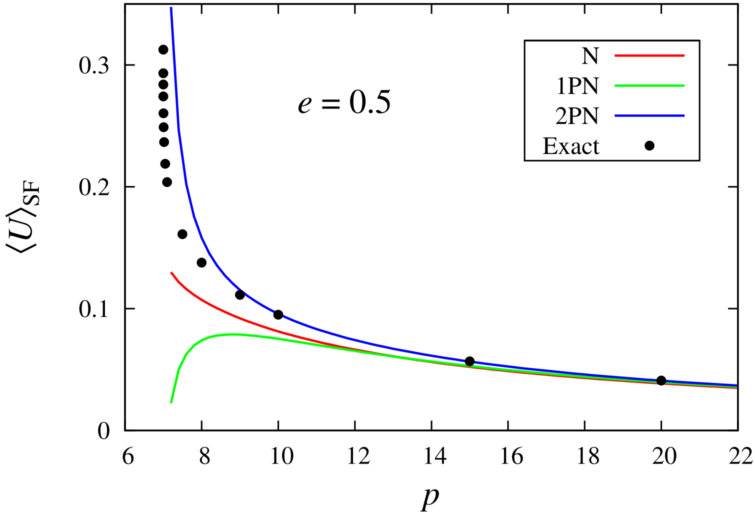

Comparison of the PN and SF results

[Barack, Le Tiec & Sago (work in progress)]

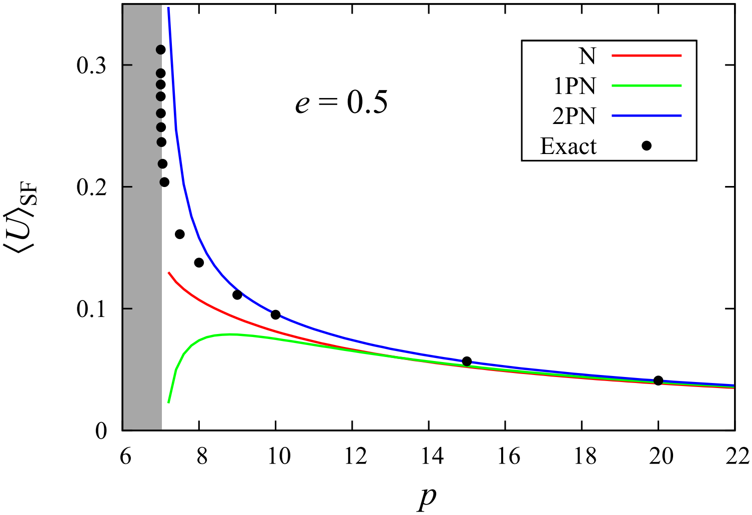

Summary and prospects

- Dissipative effects of the gravitational SF successfully tested against PN theory long ago
- More recently, comparisons with conservative SF based on: ISCO, periastron advance, redshift observable
- Comparisons relying on invariant quantities, for circular and eccentric orbits in a Schwarzschild background
- Impressive agreement between analytically determined PN coefficients and results from fit of numerical SF (e.g. 3PN)
- Extraction of previously unknown higher-order PN coefficients with high precision

Summary and prospects

- These results illustrate how the SF can tell us about PN theory in the extreme mass ratio regime

Summary and prospects

- These results illustrate how the SF can tell us about PN theory in the extreme mass ratio regime
- Many PN results are already available, and can be used for more comparisons with the gravitational SF:
  - Post-SF terms in binding energy E, energy flux $\mathcal{F}$, etc.
  - SF effects for circular/eccentric (non-)equatorial orbits in Kerr
  - ...

Summary and prospects

- These results illustrate how the SF can tell us about PN theory in the extreme mass ratio regime
- Many PN results are already available, and can be used for more comparisons with the gravitational SF:
  - Post-SF terms in binding energy E, energy flux $\mathcal{F}$, etc.
  - SF effects for circular/eccentric (non-)equatorial orbits in Kerr
  - ...
- It would also be interesting to use PN to get insight into SF:
  - Recover the MiSaTaQuWa equation from the PN formalism
  - Occurence of GW tails in both SF and PN frameworks
  - Compute the SF analytically using the PN toolkit
  - ...

Summary and prospects

- These results illustrate how the SF can tell us about PN theory in the extreme mass ratio regime
- Many PN results are already available, and can be used for more comparisons with the gravitational SF:
  - Post-SF terms in binding energy E, energy flux $\mathcal{F}$, etc.
  - SF effects for circular/eccentric (non-)equatorial orbits in Kerr
  - . . .
- It would also be interesting to use PN to get insight into SF:
  - Recover the MiSaTaQuWa equation from the PN formalism
  - Occurence of GW tails in both SF and PN frameworks
  - Compute the SF analytically using the PN toolkit
  - . . .

Prospect for a fruitful activity and many collaborations at the interface between the gravitational SF and the PN formalism